Research Article

Received: 23 June 2024 Revised: 24 October 2024 Published online in Wiley Online Library: 26 November 2024

(wileyonlinelibrary.com) DOI 10.1002/jsfa.14048

The effect of enzymatic deamidation on the solubility and emulsifying properties of walnut protein isolate

Jing Xue,[a,b,†] Sisi Feng[a,b,†] and Zheng Zhou[a,b,*]

Abstract

BACKGROUND: Alkaline-extracted walnut protein isolates (WPI) exhibit limited solubility, which poses challenges for their application in the food industry. The present study investigated the effects of protein-glutaminase (PG) deamidation on the physicochemical characteristics, solubility and emulsifying properties of WPI.

RESULTS: The deamidation process of WPI was monitored by assessing the release of free ammonia and the reduction in solution turbidity. PG deamidation significantly increased the surface charge of WPI and modified its surface hydrophobicity with increasing deamidation degree (DD), resulting in a gradual improvement in solubility by approximately 50–70%. Furthermore, the emulsifying capacity of deamidated WPI (DeWPI), specifically at 0.25 h (DeWPI0.25, DD 7%) and 9 h (DeWPI9, DD 23%), was evaluated for stabilizing low internal phase emulsions (LIPEs) and high internal phase emulsions (HIPEs). LIPEs stabilized by WPI and DeWPI0.25 exhibited significant flocculation of oil droplets, leading to decreased stability against heat, salt treatment and storage compared to those stabilized by DeWPI9. DeWPI-stabilized HIPEs showed a 2–2.5-fold higher storage modulus compared to those stabilized by WPI. However, HIPEs stabilized by DeWPI0.25 displayed higher flow stress and flow strain compared to DeWPI9-stabilized HIPEs. Overall, DeWPI-stabilized HIPEs demonstrated relatively high physical stability against storage, heat treatment and high ionic strength.

CONCLUSION: PG deamidation significantly enhanced the solubility and influenced the emulsifying properties of WPI in a manner dependent on the DD.

Supporting information may be found in the online version of this article.

Keywords: walnut protein isolates; deamidation; solubility; emulsifying properties

INTRODUCTION

In light of sustainability, health and ethical considerations, plant proteins are gaining heightened attention as primary alternatives to animal proteins.[1,2] Although there has been extensive research on widely consumed soybean, pea and other legume proteins, the exploration of nut and oilseed proteins is lacking. Walnuts are among the most widely cultivated tree nuts in the world, with significant production in countries such as China, the USA, Iran and Turkey. Walnut protein, a sustainable and potentially valuable source of protein derived from walnut oil processing byproducts, has been largely overlooked despite its global importance.[3] The conventional method for walnut protein isolate (WPI) production involves alkaline extraction and acid precipitation.[4] In addition, alternative approaches such as salt extraction and reverse micellar extraction have been reported.[5] However, the extracted WPI demonstrated limited solubility, leading to unfavorable emulsifying capabilities. Therefore, it is challenging to enhance the solubility and functionalities of WPI aiming to broaden its application in the food industry.

Physical and chemical modifications can generally influence the basic physicochemical properties of food proteins and alter their emulsifying ability.[1] Various physical, chemical and enzymatic treatments have been shown to enhance the solubility and functionality of walnut proteins.[6,7] Several techniques, including high-speed shearing, ultrasonic treatment and high hydrostatic pressure processing, have been documented to improve the solubility and emulsifying ability of WPI to varying degrees.[8-10] Chemical modifications such as glycosylation and oxidation can have contrasting effects on WPI functionality. Although these treatments often impair solubility, they can also enhance emulsifying ability under specific conditions.[11,12] Our previous studies have shown that the phosphorylation of walnut proteins by

* *Correspondence to: Z Zhou, Room 403, School of Food Science and Bioengineering, Xihua University, Chengdu, 610039, China. E-mail: zhouzheng-cn@outlook.com*

† *These authors contributed equally.*

a *School of Food Science and Bioengineering, Xihua University, Chengdu, China*

b *Chongqing Key Laboratory of Speciality Food Co-Built by Sichuan and Chongqing, Chongqing, China*

sodium tripolyphosphate or sodium trimetaphosphate significantly increases the surface charge and improves the solubility by introducing negatively charged phosphoryl groups.[13,14] Moreover, covalent conjugation of epigallocatechin-3-gallate and ellagic acid produces similar effects at the same time as additionally enhancing the emulsifying ability and antioxidant capacity of the polyphenol–WPI conjugate.[15] However, it is crucial to note that these chemical modification methods inevitably impact protein digestibility and may introduce toxicity concerns.[16]

Protein deamidation involves the alteration of amide groups in asparagine and glutamine residues.[17] However, due to the limited availability of suitable enzymes in the early days, most related work has been conducted in diluted alkaline or acidic solutions at elevated temperatures, leading to protein hydrolysis.[18] Protein glutaminase (PG) is a specific enzyme that catalyzes the conversion of the amino acid glutamine into glutamate and ammonia.[19] This process increases the content of negatively charged glutamate residues in food proteins and potentially improves their solubility. Deamidation using PG has been reported to significantly enhance the solubility of various proteins, including zein, oat protein, pea protein and coconut protein.[20-23] This enhanced solubility and altered protein characteristics generally facilitate a concomitant improvement in their emulsifying and foaming abilities.[18] Additionally, deamidation might also influence the flavor-binding capacity of proteins, potentially leading to enhanced flavor profiles in food products.[24,25] Overall, compared to other physical and chemical modification strategies, enzymatic deamidation is undoubtedly a convenient, moderate and energy-saving method. However, whether it can effectively address the challenges associated with walnut proteins remains unknown. It is worth noting that the extent of solubility improvement is normally dependent on the degree of deamidation (DD).[26,27]

Furthermore, the potential effects of DD on the properties of low and high internal phase emulsions stabilized by deamidated walnut protein remain understudied. Plant proteins are nutritional macromolecular emulsifiers for stabilizing emulsions. The physical stability of plant protein-stabilized low internal phase emulsions (LIPEs) is primarily attributed to electrostatic repulsions and steric hindrance among oil droplets from the surface-covered proteins.[28] For high internal phase emulsions (HIPEs), rheological properties are key features influencing their application as dressings, alternatives to partially hydrogenated oils, or 3D printing materials.[29] These rheological properties are also significantly influenced by the characteristics of the interface-adsorbed proteins. Deamidation is expected to significantly alter the surface charges, particle sizes and surface hydrophobicity of walnut proteins, resulting in distinct physical stability and rheological properties of the stabilized emulsions.

The present study aimed to explore the influence of enzymatic deamination by protein glutaminase on the physicochemical properties, solubility and emulsifying properties of walnut proteins. The time-dependent deamidation of walnut proteins was evaluated by monitoring the release of free ammonia and the decrease in turbidity due to improved protein solubility. The influence of different deamidation degrees (DD) on the surface charge, surface hydrophobicity and solubility was also examined. Moreover, the emulsifying ability of deamidated walnut protein isolate (DeWPI) with different DD to stabilize LIPEs and HIPEs was comprehensively investigated. These findings highlight an effective and convenient method for enhancing the solubility and emulsifying ability of WPI, thereby potentially expanding the applications of walnut protein sources in the food industry.

MATERIALS AND METHODS

Materials

Raw walnut kernels (cultivar WEN185) were harvested from Kuche Couty, Xinjiang Province, China. Protein glutaminase (500 U g^{-1}) was kindly provided by Amano Enzyme Inc. (Nagoya, Japan). Medium-chain triglyceride (MCT) was purchased from Yuanye Bio-Technology (Shanghai, China). A bicinchoninic acid (BCA) protein assay kit and *o*-phthaldialdehyde (OPA) were obtained from Sangon Biotech Co., Ltd (Shanghai, China). 1-Anilinonaphthalene-8-sulfonate (ANS) was obtained from Sigma-Aldrich (St Louis, MO, USA). All other chemical reagents were of analytical grade and obtained from Kelong Chemical Co., Ltd (Chengdu, China).

Alkaline extraction of WPI

WPI was prepared according to the alkaline extraction and acid precipitation method, as described by Mao and Hua.[30] Briefly, the pellicles of walnut kernels were manually removed to minimize the influence of polyphenols before grinding and defatting with *n*-hexane. The defatted walnut meal was suspended in double-distilled water (ddH_2O) at a ratio of 1:20 (w/v), and the pH was adjusted to 11.0 with 1 M NaOH. The extraction was carried out in a rotator at 25 °C for 2 h. The suspensions were then centrifuged at 10 000 × *g* for 30 min at room temperature, and the precipitates were re-extracted as described above. The combined supernatants were mixed and precipitated by adjusting the pH to 4.5 with 1 M HCl. The resulting centrifuged precipitates were resuspended in ddH_2O, and the pH was adjusted to 7.0, followed by freezing and lyophilization.

Turbidity measurements

The WPI was suspended in ddH_2O at a concentration of 10 g L^{-1}, and the temperature was maintained at 37 °C using a circulating water bath. Subsequently, 5 U g^{-1} of protein glutaminase (0.1 g L^{-1}) was rapidly added, and the turbidity, reflected as the UV absorbance at 500 nm, was recorded during the deamidation process using a UV2600i spectrometer (Shimadzu Corporation, Kyoto, Japan).

Determination of DD

The DD of the WPI was determined by calculating the ratio of the released free ammonia to the total ammonia released from the hydrolyzed WPI. The amount of released ammonia was quantified using the fluorescent OPA method.[31] At specific incubation time points during deamidation, samples (200 μL) were taken and mixed with 600 μL of 20% trichloroacetic acid, followed by incubation on ice for 15 min to precipitate proteins. Subsequently, the samples were centrifuged at 10 000 × *g* for 10 min, and the supernatant was combined with the OPA reagent [freshly prepared by mixing 40 mg of OPA in 1 mL of methanol, 20 mL of 100 mM borate buffer, pH 10.0, 2.5 mL of 100 g L^{-1} sodium dodecyl sulfate (SDS) and 100 μL of 5 mM dithiothreitol and making up to 100 mL with ddH_2O] and incubated for an additional 10 min. The fluorescence intensity at 420 nm of the samples with an excitation wavelength of 360 nm was recorded using an RF6000 spectrofluorometer (Shimadzu Corporation). The amount of free ammonia was then determined using a standard curve of NH_4Cl solutions ranging from 0 to 100 μM. Meanwhile, WPI was hydrolyzed using 6 M HCl at 110 °C for 24 h, and the total amount of released ammonia was quantified using the OPA method as described above.

Preparation of deamidated walnut proteins

Enzymatic deamidation of WPI was performed by the addition of 5 U g^{-1} protein glutaminase to 10 g L^{-1} WPI suspension. The suspension was incubated at 37 °C for 0.25, 2 and 9 h. The deamidation process was stopped by treating the samples at 85 °C for 10 min. The deamidated walnut proteins were dialyzed against ddH_2O to remove the released ammonia for 48 h with at least four times changing of water. The dialyzed protein suspensions were then lyophilized. The deamidated walnut proteins subjected to different treatment durations (0.25, 2 and 9 h) were designated as DeWPI0.25, DeWPI2 and DeWPI9, respectively.

Surface hydrophobicity assay

The surface hydrophobicity of DeWPI was assessed using the protein hydrophobic region-specific dye ANS.[32] Protein samples were suspended in ddH_2O and diluted to concentrations ranging from 0.05 to 0.5 g L^{-1}. Then, 8 mM ANS stock solution was added to achieve a final concentration of 100 μM. The fluorescence intensity of ANS at 480 nm when excited at 360 nm was recorded using an RF6000 fluorescence spectrometer (Shimadzu Corporation). The slope of the linear fit of ANS intensity to protein concentration was used as the surface hydrophobicity index (H_0).

Size and zeta potential measurements

The changes in the particle size and zeta potential of the DeWPI were measured using a NanoZS Zetasizer analyzer (Malvern Instruments Ltd, Malvern, UK) equipped with a 633 nm laser, operating at 25 °C. Protein samples were prepared in 20 mM sodium phosphate buffer (pH 7.0) at a concentration of 1 g L^{-1}. The refractive and absorption indices of the particles were set at 1.450 and 0.001, respectively. The particle size was expressed as *Z*-average diameter.

Intrinsic fluorescence spectroscopy

The protein samples were prepared in 20 mM phosphate buffer (pH 7.0) to a final concentration of 0.3 g L^{-1}. The samples were excited at a wavelength of 280 nm, and emission wavelengths ranging from 290 to 450 nm were recorded using an RF6000 fluorescence spectrometer (Shimadzu Corporation). Both the excitation and emission slit widths were set at 3.0 nm.

Circular dichroism (CD)

The protein samples were prepared in 20 mM phosphate buffer (pH 7.0) to a final concentration of 0.3 g L^{-1}. CD spectra of the samples and buffer were recorded from 190 to 260 nm using a Chirascan100 CD spectrometer (Applied Photophysics Ltd, Leatherhead, UK).

Determination of protein solubility

The WPI and DeWPI samples were suspended in 20 mM phosphate buffer (pH 7.0) to a concentration of 10 g L^{-1} and allowed to stand at room temperature for 3 h. Subsequently, the samples were centrifuged at 10 000 × *g* for 30 min to separate undissolved proteins, and the solubilized proteins were quantified using a BCA protein quantification kit. The protein solubility was calculated as the percentage of the concentration of solubilized protein in the supernatant relative to the initial total protein concentration.

Preparation of emulsions

The WPI and DeWPI samples were prepared at a concentration of 10 g L^{-1} in 20 mM phosphate buffer containing 0.02% NaN_3 (pH 7.0). MCT oil served as the dispersed phase, with protein dispersions added at a volume ratio of 1:9. The mixed samples underwent high-speed shearing at 15 000 rpm for 2 min using a T25 digital dispersing instrument (IKA Instruments, Staufen in Breisgau, Germany) to form coarse emulsions. Subsequently, the coarse emulsions were passed four times through a NanoGenizer 45 K high-pressure homogenizer (Genizer, Irvine, CA, USA) operating at 100 MPa to produce fine emulsions.

For the preparation of HIPEs, the concentration of WPI and DeWPI was increased to 20 g L^{-1} to accommodate the higher oil phase content. The internal phase (MCT oil at a volume fraction of 80%) was mixed with the WPI and DeWPI dispersions. This mixture was then homogenized using a T18 high-speed homogenizer (IKA Instruments) at 10 000 rpm for 2 min.

Oil particle size distribution measurements

LIPEs or HIPEs prepared with WPI and DeWPI emulsifiers were suspended in ddH_2O or 10 g L^{-1} SDS (to inhibit oil droplet flocculation caused by hydrophobic interactions). The dispersed samples were then added to the circulation chamberuntil the shading rate reached approximately 10% before the data were collected using a Bettersizer 2600 laser diffraction particle size analyzer (Bettersize Instrument Co., Dandong, China). The pump speed was set at 1200 rpm. The refractive indices of water and oil were set to 1.33 and 1.52, respectively.

The particle size was expressed as the volume-weighted mean diameter ($d_{4,3}$). The flocculation index (FI) was calculated using:

$$FI = (d_{4,3\ water} - d_{4,3\ SDS})/d_{4,3\ SDS}$$

where $d_{4,3\ water}$ and $d_{4,3\ SDS}$ are the $d_{4,3}$ values obtained from measurements in water and in 10 g L^{-1} SDS, respectively.[33]

Emulsion morphology observation

For LIPEs, the emulsion samples were diluted 10 times with phosphate buffer, stained with Nile red (1 g L^{-1}, dissolved in ethanol), excited at 488 nm and imaged using a CLSM600 confocal laser scanning microscope (Sunny Optical Technology, Suzhou, China) with a 100× objective. For HIPEs, the oil phase was prestained with Nile red (1 g L^{-1}, dissolved in ethanol) and the continuous phase was prestained with Nile blue A (1 g L^{-1}, dissolved in ethanol). Then, the HIPEs were prepared as described in the section above on 'Preparation of emulsions' and observed using a confocal laser scanning microscope equipped with a 20× objective. Nile red was excited at 488 nm and Nile blue A was excited at 640 nm. In addition, the morphology of the emulsion oil droplets was also imaged under a differential interference contrast model using the CLSM600 microscope.

Rheological analysis

Rheological measurements were performed using an MCR302 rheometer (Anton Paar, Graz, Austria) with a PP25 parallel plate geometry (gap of 1 mm) at a constant temperature of 25 °C. Amplitude sweep experiments were conducted at a fixed frequency of 1 Hz, and the strains were scanned from 0.1% to 300%. The flow strains and flow stresses corresponding to the strain and stress at the crossover of the storage modulus (G') and loss modulus (G'') were calculated using RheoCompass, version 3.1 (Anton Paar). Frequency sweeps were conducted at a fixed strain of 0.5% within the linear viscoelastic region (LVR) and frequencies ranging from 0.1 to 10 Hz. Loss factors (tan δ) were calculated by G''/G'.

Evaluation of emulsion stability

To evaluate the thermal stability, the emulsions were subjected to thermal treatments at 60 and 90 °C for 30 min and then cooled to room temperature.

The influence of ionic strength on the stability of LIPEs was investigated by adding 5 M NaCl stock solution to achieve final concentrations of 150 and 300 mM. For HIPEs, protein emulsifiers were suspended in 20 mM phosphate buffer (pH 7.0) supplemented with 150 and 300 mM NaCl before preparation.

The emulsions were also stored at room temperature for 28 days to evaluate their long-term stability.

After treatment, the oil particle size distribution and zeta potential were measured as described in the section above on 'Oil particle size distribution measurements'. The rheological properties of the HIPEs were also characterized.

Statistical analysis

All experiments were conducted at least in triplicate. Statistical analysis was performed using SPSS, version 10 software (SPSS Inc., Chicago, IL, USA) and the significance of each group was assessed using one-way analysis of variance followed by Duncan's new multiple-range method for post-hoc analysis.

RESULTS AND DISCUSSION

Alterations in turbidity and DD

As shown in Fig. 1(A), a time-dependent decrease in the absorbance of WPI at 500 nm wavelength was observed during the PG deamidation reaction. Initially, the absorbance of the WPI dispersion was approximately 3.2, indicating its poor solubility and high turbidity. Within the first 30 min, the absorbance of the dispersion decreased significantly to approximately 0.5. Subsequent incubation for 1–2 h resulted in a slower decrease in absorbance, eventually reaching a plateau of approximately 0.15, indicating increased transparency of the system (see Supporting information, Fig. S1). The decrease in turbidity suggested that PG deamidation could effectively enhance the solubility of the WPI. Based on the above results, the increase in the DD of DeWPI throughout the reaction time was further monitored and is depicted in Fig. 1(B). Consistent with the results of the turbidity assay, the DD sharply increased to approximately 16% within the initial 2 h. This observation aligns with previous research demonstrating a significant decrease in turbidity with increasing DD in α-zein and wheat gluten dispersions.[20,34] However, although the turbidity of WPI decreased to a stable level, the DD continued to increase noticeably. Deamidation of WPI to a level of approximately 16% appeared to be sufficient to achieve significantly enhanced aqueous solubility. However, prolonged incubation times led to continued enzymatic activity on the protein substrate, resulting in the further conversion of glutamine to glutamate. The rate of DD increase decelerated after 2 h, reaching a plateau of approximately 24% at 12 h.

Effect of deamidation on physicochemical properties of WPI

The influence of varying DD on the physicochemical properties of WPI was studied in detail. As shown in Fig. 2(A), the zeta potential of DeWPI progressively increased by approximately 8 mV (from −30.4 to −38.5 mV) as the deamidation time increased from 0 to 9 h. This increase can be attributed to the rise in the amount of negatively charged glutamate.[19] Enzymatic deamidation also significantly enhanced the zeta potential of pea protein isolates and wheat gluten.[24,35] As shown in Fig. 2(B), a significant increase in the surface hydrophobicity of DeWPI was observed after deamidation for short durations (DD 7–16%). However, this trend reversed with a further reaction time of 9 h (DD 23%), leading to a decrease in surface hydrophobicity. Deamidation could increase the surface charge and solubility of proteins, leading to the dissociation of protein aggregates and exposure of the internal buried hydrophobic region, which contributed to the initial increase in hydrophobicity.[36,37] However, prolonged deamidation might induce conformational changes in the protein structure and increased negative charges from glutamate residues, potentially disrupting hydrophobic regions formed with neighboring amino acids. Zhao *et al.*[38] also observed a similar phenomenon, where limited deamidation significantly increased the surface hydrophobicity of hordein. However, a further increase in the DD resulted in a substantial decrease in surface hydrophobicity.

Conformational changes in WPI upon deamidation

The intrinsic fluorescence, which is sensitive to the local environment of chromophores such as tryptophan (Trp) and tyrosine (Tyr) is often used to reflect the alterations in the tertiary structure of proteins. As shown in Fig. 2(C), the peak wavelength of WPI was

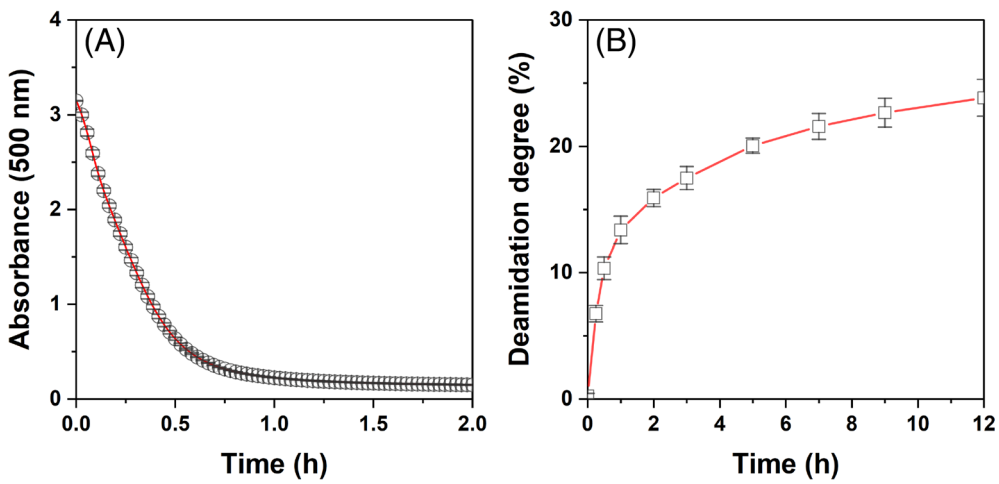

Figure 1. Time-dependent decrease in turbidity (evaluated as absorbance at 500 nm) (A) and increase in deamidation degree (B) of walnut protein isolates treated with protein-glutaminase.

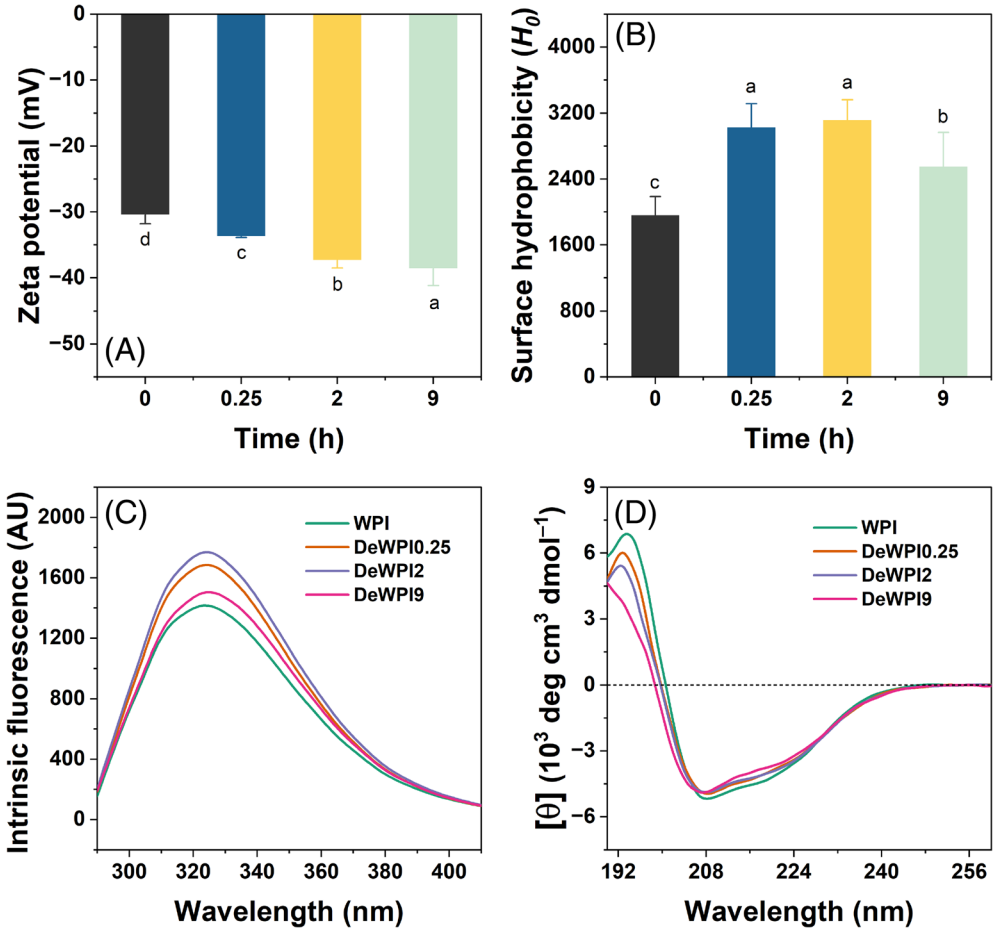

Figure 2. The effects of deamidation time on the zeta potential (A) and surface hydrophobicity (B) of the protein-glutaminase-deamidated walnut protein isolates (WPI). Different letters indicate statistically significant differences ($P < 0.05$). (C) Intrinsic fluorescence and (D) circular dichroism spectra of WPI and deamidated WPI (DeWPI) at different treatment times (0.25, 2 and 9 h).

approximately 323 nm, suggesting a compact folded protein structure with internal buried hydrophobic amino acid residues. After deamination for 0.25 and 2 h, the intrinsic fluorescence intensity of DeWPI with a DD of 7–16% increased significantly, whereas the peak wavelength remained unchanged. This indicated that the hydrophobic Trp residues were partially exposed as a result of the dissociation of protein aggregates, which was consistent with the enhanced surface hydrophobicity.[39,40] Extending deamidation to 9 h resulted in a decrease in the intrinsic fluorescence intensity of the protein. Additionally, a slight redshift of the peak wavelength at 325 nm was observed. This combined effect was likely attributable to the partial unfolding of the deamidated WPI with a DD of 23%, potentially exposing tryptophan residues to a more hydrophilic environment.[41]

CD spectra can provide insights into the secondary structural changes of proteins. As shown in Fig. 2(D), the CD spectra of WPI displayed a positive peak at 195 nm and double negative peaks at 208 nm and 222 nm. With increasing DD, the spectra of DeWPI exhibited a gradual decrease in the intensity of the positive peak at 195 nm and the negative peak at 222 nm. Additionally, the negative peak at 208 nm slightly blueshifted to 206 nm, which was especially pronounced in the DeWPI9. These alterations in the CD spectra indicated a progressive loss of the α-helix content of WPI during the deamidation process. *In silico* analysis of the predicted secondary structures (see Supporting information, Table S1) revealed a gradual decrease in the α-helix content from 8.9% for native WPI to 8% after 9 h of deamidation. Conversely, the β-sheet content increased from 35.3 to 36.6% ($P < 0.05$). PG-deamidated α-zein and coconut protein also showed a declined α-helix content and an increased β-sheet structure.[20,23] Notably, enzymatic deamidation of WPI resulted in relatively smaller changes in fluorescence and secondary structure compared to those of the harsher chemical methods using alkaline or acidic treatment. This suggested that enzymatic deamidation offered a more moderate approach, potentially minimizing protein denaturation and hydrolysis.[18] SDS-polyacrylamide gel electrophoresis results (see Supporting information, Fig. S2) indicated that major protein bands in WPI remained unchanged after deamidation, further confirming the minimal hydrolysis of protein components in WPI.

Protein solubility analysis

The impact of deamidation on the solubility of WPI was investigated. As shown in Fig. 3(A), at a reaction time of 0.25 h (DD of approximately 7%), the solubility of DeWPI exhibited a significant increase from approximately 30% to more than 75%. With prolonged incubation times of 2–9 h (DD ranged from 16 to 23%), the solubility of DeWPI further increased to almost 100%. Additionally, Fig. 3(B) illustrates the changes in the particle size of WPI during the deamidation process. The initial WPI sample

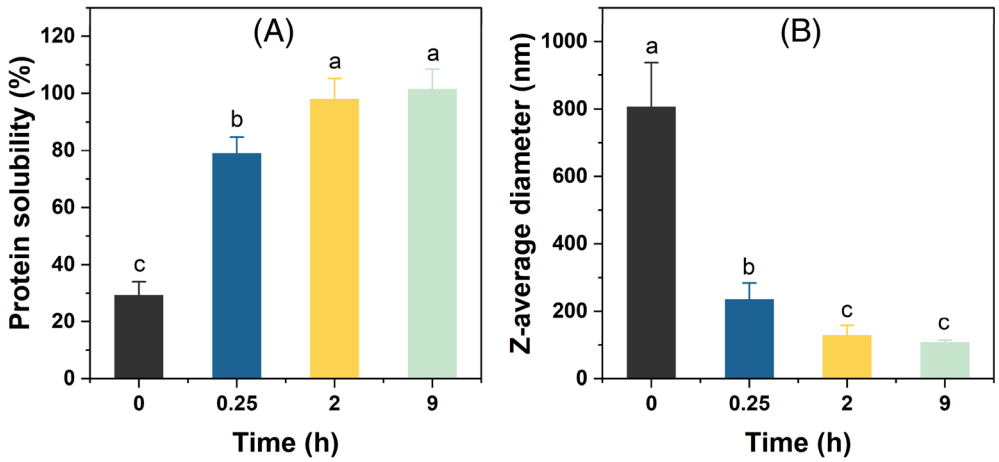

Figure 3. The effects of deamidation time on the protein solubility (A) and Z-average diameter (B) of the protein-glutaminase-deamidated walnut protein isolates. Different letters indicate statistically significant differences ($P < 0.05$).

showed a large mean particle size of more than 800 nm, which notably decreased to approximately 200 nm after reacting for 0.25 h and further decreased to approximately 100 nm after reacting for 2–9 h. These findings collectively indicated that enzymatic deamidation was an effective method for enhancing the solubility and dispersity of WPI. Jang *et al.*[26] reported that PG deamidation effectively improved the solubility of oat protein isolate (OPI), particularly at a DD of 44–59%. Interestingly, wheat gluten exhibited significantly enhanced solubility even at a lower DD of 23%.[34] This observation aligns with the findings in the present work, where WPI also showed significant improvement in solubility at a moderate deamidation level. This might be associated with the intrinsic characteristics of the proteins, such as their structural features and amino acid composition, which can influence their susceptibility to deamidation-induced changes in physicochemical properties. According to previous studies, wheat gluten, primarily composed of gliadins and glutenin proteins, had a high content of glutamic acid plus glutamine (Glx) of 37.5%,[42] with glutamine existing as polyglutamine sequences,[43] making it an ideal substrate for PG deamidation. The low solubility of OPI is primarily attributed to the association and aggregation of its high content of globulin proteins. Although previous studies frequently reported gluten as the most abundant protein fraction in WPI, mass spectrometry identification revealed vicilin and legumin-like globular proteins as the main components of WPI.[8] Glx are also the dominant amino acids in OPI and WPI, with a content of approximately 24%.[8,44] Notably, OPI exhibits a significantly higher content of hydrophobic amino acids compared to WPI (38.7 *versus* 29%), suggesting that a higher DD is necessary for improved solubility. In addition, the accessibility of glutamine residues within the protein molecules also influences deamidation effects.

In conclusion, enzymatic deamidation can effectively enhance the solubility and modulate the hydrophilic–hydrophobic balance of walnut proteins, potentially influencing their emulsifying abilities. To investigate this possibility, the emulsifying properties of DeWPI with a relatively low DD of 7% (deamidated for 0.25 h; DeWPI0.25) and a higher DD of 23% (deamidated for 9 h; DeWPI9) were comparatively evaluated in subsequent studies.

Microstructure, particle size and zeta potential of LIPEs

LIPEs containing 10% MCT oil were prepared using WPI, DeWPI0.25 and DeWPI9. The confocal laser scanning microscopy (CLSM) images in Fig. 4(A) revealed significant oil droplet flocculation within the WPI- and DeWPI0.25-stabilized LIPEs. Conversely, DeWPI9-stabilized LIPEs exhibited relatively well-dispersed oil droplets. This observation aligned with the size distribution data (Fig. 4B,C). WPI- and DeWPI0.25-stabilized LIPEs displayed a multimodal distribution with two main peaks, indicating a wider range of droplet sizes. By contrast, the DeWPI9-stabilized LIPEs displayed a single peak, suggesting a more uniform size distribution. The $d_{4,3}$ values for the WPI- and DeWPI0.25-stabilized LIPEs were approximately 9.2 μm and 5.6 μm, respectively. Notably, DeWPI9-stabilized LIPEs exhibited a significantly smaller mean droplet size of approximately 0.81 μm (Fig. 4D). Interestingly, when suspended with SDS, the difference in $d_{4,3}$ values between WPI- and DeWPI-stabilized LIPEs diminished (Fig. 4E). This suggests that SDS disrupts hydrophobic interactions, leading to well-separated oil droplets in all emulsions. FI analysis corroborated these observations (Fig. 4F). The WPI-stabilized LIPEs exhibited an FI of 9.37, which was approximately 1.5-fold that of the DeWPI0.25-stabilized LIPEs and 25 times higher than that of the DeWPI9-stabilized LIPEs. Despite SDS treatment, the oil droplets in the WPI-stabilized LIPEs remained approximately 300 nm larger than those in the DeWPI9-stabilized LIPEs. However, flocculation appeared to be the primary factor influencing overall emulsion physical stability. Zeta potential measurements (Fig. 4G) revealed a lower negative charge (−32 mV) for the oil droplets in the WPI-stabilized emulsions than in the DeWPI-stabilized emulsions (−38 mV). This higher negative charge in DeWPI-stabilized emulsions implied stronger electrostatic repulsion among oil droplets, potentially contributing to their improved stability. Notably, DeWPI0.25-stabilized LIPEs exhibited similar oil droplet charges as DeWPI9-stabilized LIPEs. However, the higher surface hydrophobicity of DeWPI0.25 might explain the observed flocculation. Previous studies have also demonstrated that DD influenced the enhancement of emulsion properties in enzymatically deamidated coconut protein and oat protein.[23,26] Deamidation likely improved the emulsifying ability of WPI through several mechanisms. First, the enhanced solubility of DeWPI increased the availability of protein emulsifiers for adsorption at the oil–water interface. Second, the enhanced surface charge of DeWPI could significantly impact the characteristics of the resulting oil droplets.

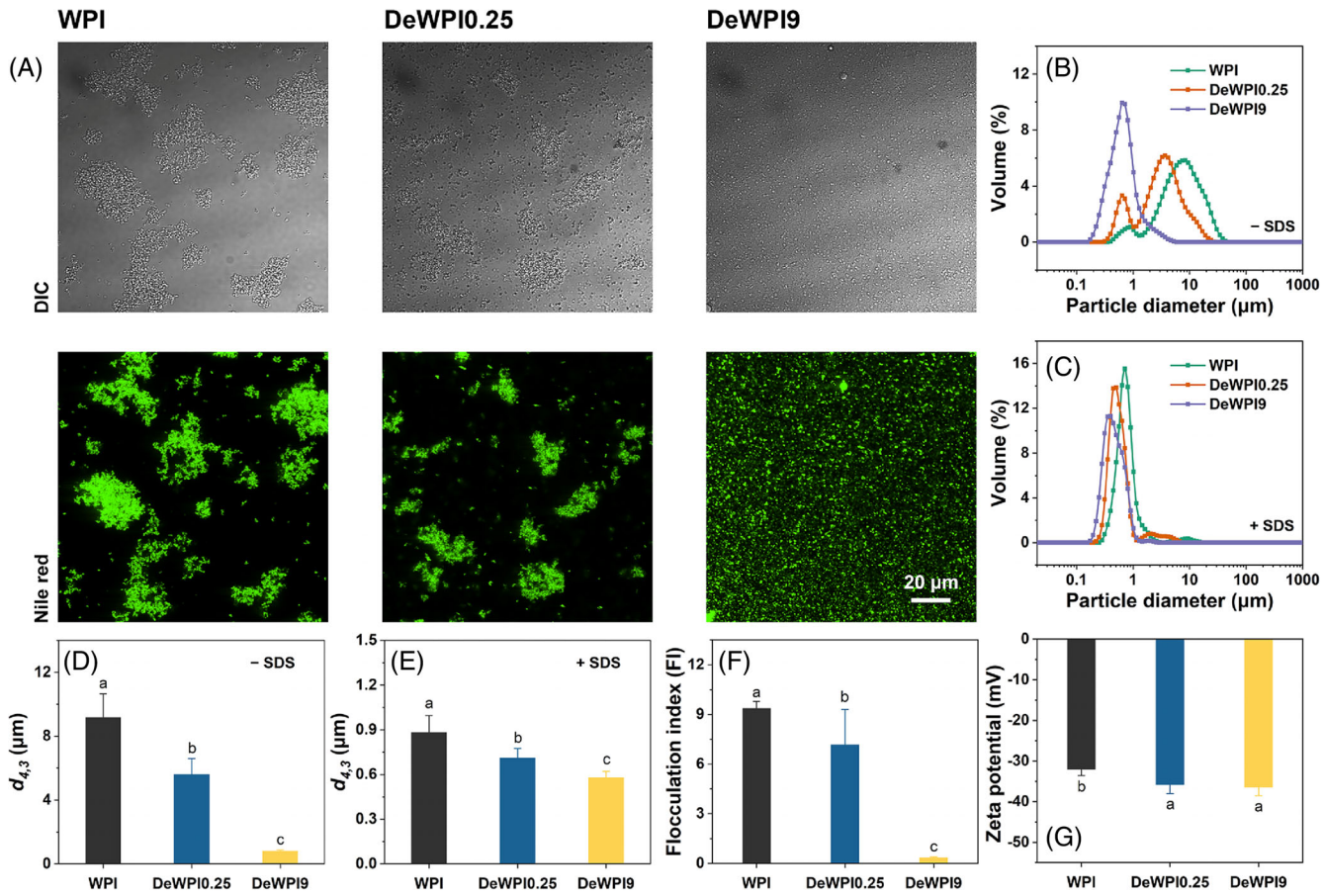

Figure 4. (A) CLSM images of oil droplets stained with Nile red in the low internal phase emulsions (LIPEs) stabilized by walnut protein isolates (WPIs), DeWPI0.25 and DeWPI9. (B,C) Size distribution of the oil droplets in the emulsions dispersed with ddH_2O (−SDS) or 10 g L^{-1} SDS (+SDS). (D, E) Volume-weighted mean diameter ($d_{4,3}$) determined with ddH_2O or 10 g L^{-1} SDS. (F) Flocculation index and (G) zeta potential of the oil droplets in the emulsions. Different letters indicate statistically significant differences ($P < 0.05$).

Physical stability of LIPEs stabilized by DeWPI

The stability of the emulsions under heat, salt and storage conditions was evaluated and the results are shown in Fig. 5. The influence of long-term storage on the $d_{4,3}$ of DeWPI9-LIPEs was limited (Fig. 5A). Storage for 28 days did not significantly alter the surface charge of the oil droplets (Fig. 5D). However, the measured $d_{4,3}$ values of the LIPEs stabilized by WPI significantly increased with prolonged incubation time (from 9.2 to 13 μm). After storage, extensive oil droplet flocculation was observed in both the WPI- and DeWPI0.25-stabilized emulsions (see Supporting information, Fig. S3). By contrast, the oil droplets in DeWPI9-stabilized LIPEs remained well-dispersed and homogeneous (see Supporting information, Fig. S3A). As shown in the Supporting information (Fig. S3B), DeWPI9-stabilized emulsions displayed superior stability throughout the incubation period, remaining homogenous, whereas WPI- and DeWPI0.25-stabilized emulsions exhibited creaming over time. The enhanced stability of the emulsions stabilized by DeWPI9 with a high DD might be attributed to increased electrostatic repulsion among the oil droplets because of their higher surface charge. This concept aligned with findings in EGCG-conjugated black bean protein emulsions, where increased surface charge contributed to improved stability.[45]

Although minimal changes in zeta potential were observed upon heating (Fig. 4B,E), the $d_{4,3}$ values of WPI- and DeWPI0.25-stabilized LIPEs significantly increased (approximately 1.4–2-fold) after heating at 90 °C for 30 min. This increase was probably a result of heat-induced protein unfolding and enhanced hydrophobic interactions, leading to oil droplet aggregation.[46] Notably, DeWPI9-stabilized LIPEs displayed superior resistance to heat treatment. The CLSM images in the Supporting information (Fig. S4A) revealed more severe flocculation of oil droplets in the WPI- and DeWPI0.25-stabilized emulsions after heat treatment. Conversely, the DeWPI9-stabilized emulsions maintained a homogenous oil droplet distribution. These observations are further confirmed in the Supporting information (Fig. S4B), with visual demonstration of slight creaming in both the WPI- and DeWPI0.25-stabilized emulsions following heat treatment. This observation aligned with previous research, where polyphenol-conjugated WPI with higher surface charge also exhibited enhanced thermal stability.[15]

Salt treatment, as expected, resulted in a decrease in the zeta potential of the oil droplets in all LIPEs (Fig. 5F) as a result of surface charge screening by the high concentration of ions.[47] This decline in electrostatic repulsion led to pronounced flocculation in WPI- and DeWPI0.25-stabilized LIPEs, as observed in the CLSM images (see Supporting information, Fig. S4A). The $d_{4,3}$ values of the WPI-stabilized emulsions increased from 9.2 to 11 μm, and that in the DeWPI0.25-stabilized emulsions increased from 5.6 μm to approximately 6.5 μm. DeWPI9-stabilized LIPEs displayed a modest increase in $d_{4,3}$ (0.8–1.75 μm) and weak signs

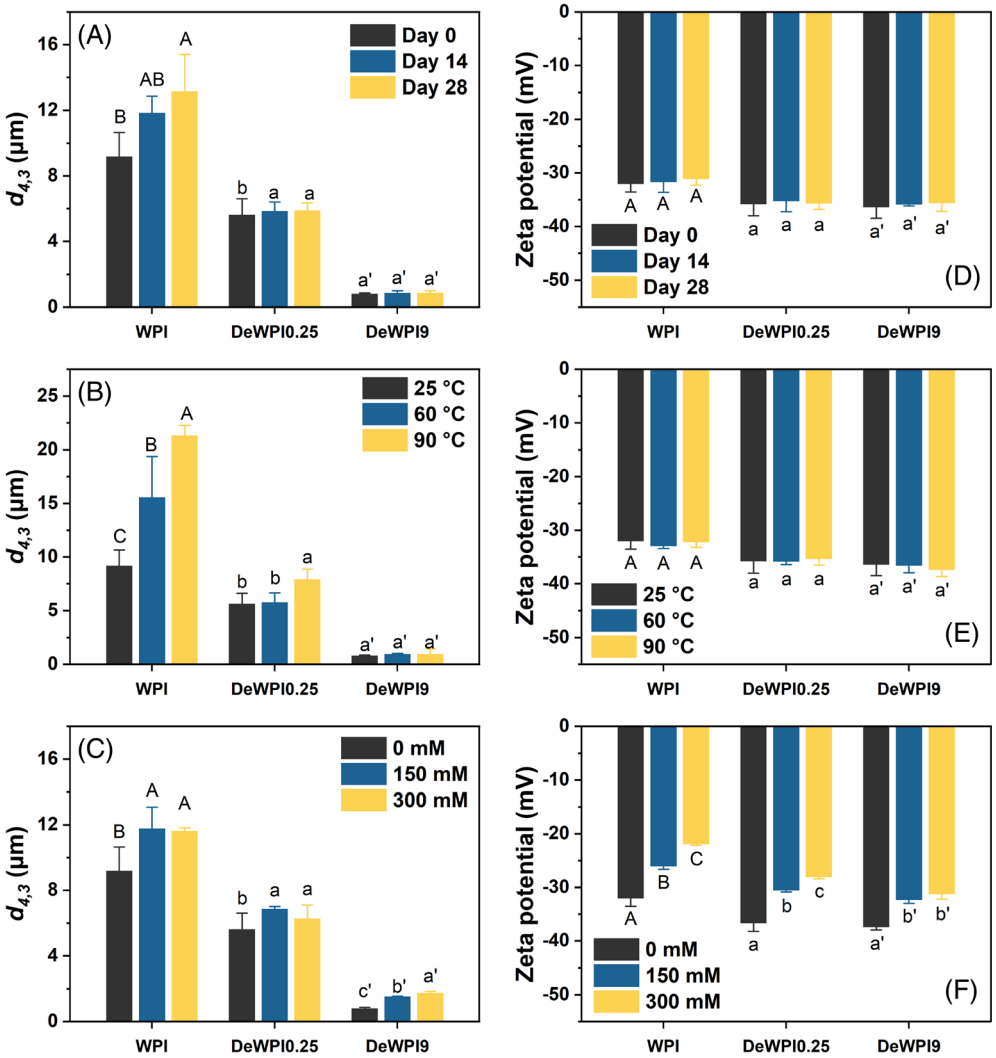

Figure 5. The influence of long-term storage (A, D), heat treatment (B, E) and high ionic strength (C, F) on the volume-weighted mean diameter ($d_{4,3}$) and zeta potential of oil droplets in the low internal phase emulsions (LIPEs) stabilized by walnut protein isolates (WPI), DeWPI0.25 and DeWPI9. Different letters indicate statistically significant differences ($P < 0.05$).

of flocculation (see Supporting information, Fig. S4A) upon exposure to 300 mM NaCl. Notably, WPI-stabilized emulsions exhibited creaming at a relatively low salt concentration (150 mM NaCl) (see Supporting information, Fig. S4B). By contrast, the DeWPI-stabilized emulsions remained stable and homogenous even at 300 mM NaCl, indicating their enhanced salt tolerance. These observations collectively suggested that deamidation, particularly to the extent observed in DeWPI9 with a DD of 23%, enhanced the emulsion stability against high ionic strength.

Microstructure, particle size and zeta potential of HIPEs

The capacity of WPI and DeWPI to stabilize HIPEs was further investigated. Both WPI and DeWPI effectively stabilized the HIPEs, as evidenced by the formation of pasty samples adhering to the bottom of the inverted test tubes (Fig. 6A, inset). Nile red staining specifically labeled the oil phase as green droplets, whereas Nile blue A staining identified proteins adsorbed at the interface as red circles, indicating the formation of O/W type HIPEs. Notably, the oil droplets in the WPI-stabilized HIPEs were significantly larger than those stabilized by DeWPI. As shown in the magnified images in the inset in Fig. 6(A), the interfacial layer surrounding the oil droplets in the DeWPI-stabilized emulsions appeared denser and more homogeneous, indicating a uniform and complete adsorption of the well-solubilized walnut proteins. Conversely, WPI-stabilized emulsions exhibited thinner interfacial membranes with distinct protein aggregates, likely attributable to the poor solubility of WPI.

HIPEs formulated with WPI exhibited significantly larger oil droplets (approximately 62 μm) than those stabilized by DeWPI0.25 and DeWPI9 (approximately 40 μm and 36 μm, respectively) (Fig. 6B,C). This observation likely stemmed from the low solubility of WPI, which limited the availability of protein emulsifiers for adsorption at the oil–water interface, particularly for the high oil content (80%) present in HIPEs. PG-deamidated wheat gluten with a moderate deamination degree can also stabilize HIPEs with relatively small oil droplet sizes.[35] The zeta potential of the oil droplets remarkably depended on deamidation time. DeWPI9-stabilized HIPEs exhibited the highest zeta potential of approximately −46.5 mV, followed by DeWPI0.25-stabilized HIPEs (−37.3 mV) and WPI-stabilized HIPEs (−35.8 mV) (Fig. 6D). This trend aligned with the extent of deamidation, suggesting that deamidation enhances the surface charge density of walnut

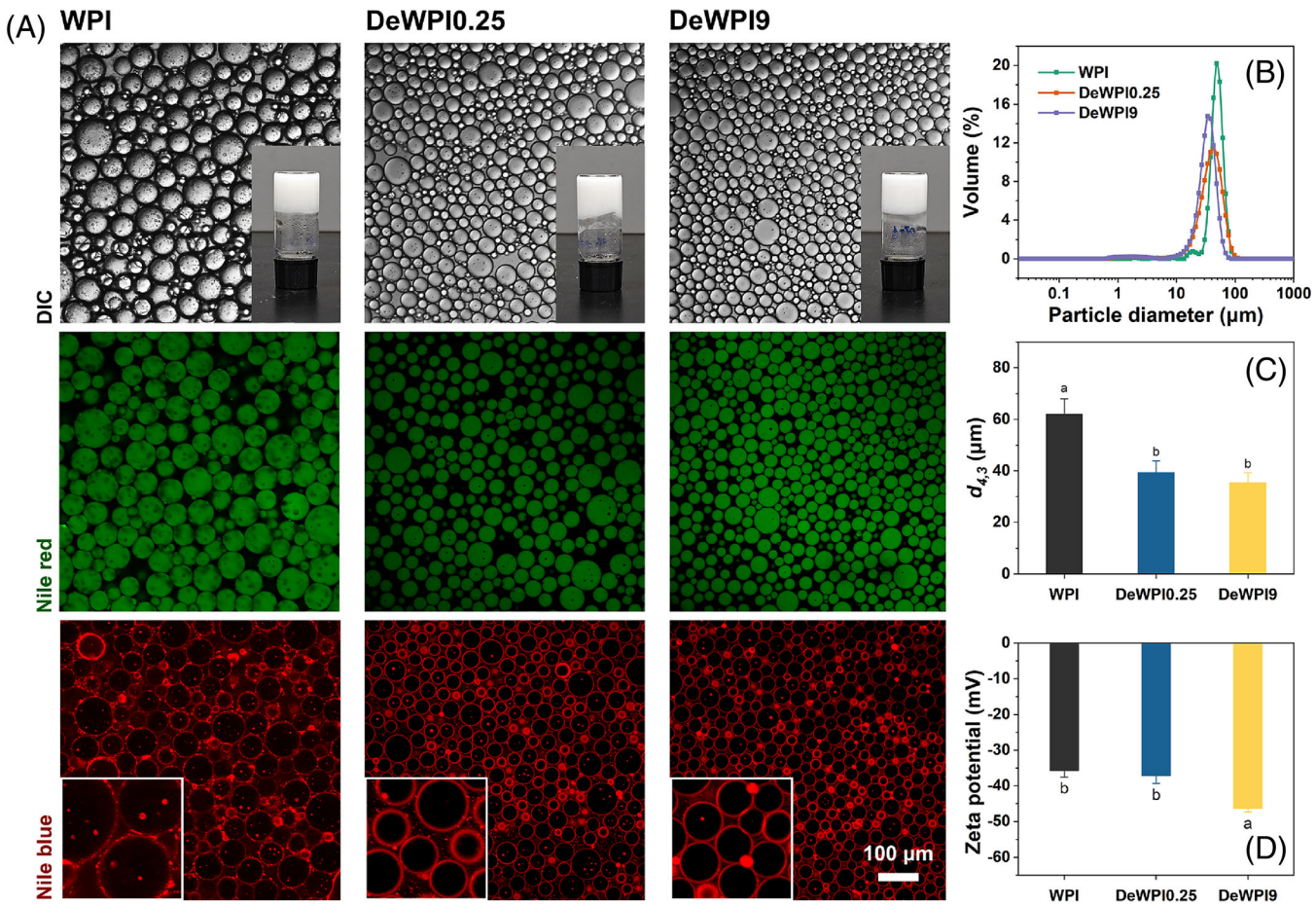

Figure 6. (A) CLSM images of oil droplets in the high internal phase emulsions (HIPEs) stabilized by walnut protein isolates (WPI), DeWPI0.25 and DeWPI9. (A, inset, top right) Visual appearance of the HIPEs. (A, inset, bottom left) Magnified images indicating the interface. (B) Size distribution, (C) volume-weighted mean diameter ($d_{4,3}$) and (D) zeta potential of oil droplets in the HIPEs. Different letters indicate statistically significant differences ($P < 0.05$).

proteins with increasing DD, leading to a greater surface charge on the covered oil droplets.

Rheological properties of the HIPEs

The rheological properties of HIPEs are crucial for determining their suitability in various applications, such as food dressings or edible inks for 3D food printing.[48] Amplitude sweep tests confirmed the viscoelastic behavior of the HIPEs (Fig. 7A). At low strains within the LVR, the storage modulus (G') remained higher than the loss modulus (G''), indicating a viscoelastic semisolid structure. Beyond the LVR, G' exhibited a gradual decrease and eventually intersected with G''. This signified a transition from elastic behavior (dominant G') to viscous behavior (dominant G''), indicating increased flowability of the material.[49] As shown in Fig. 7(B), DeWPI-stabilized HIPEs showed the highest G' of approximately 512 Pa (at a strain of 0.5% within the LVR), followed by DeWPI0.25-stabilized HIPEs (approximately 429 Pa), both of which were substantially greater than WPI-stabilized HIPEs (approximately 209 Pa). Smaller oil droplets in DeWPI-stabilized HIPEs resulted in a larger contact interfacial area among oil droplets, promoting stronger inter-droplets interactions and leading to more elastic emulsions.[50] Compared with the DeWPI9-stabilized HIPEs, the DeWPI0.25-stabilized HIPEs exhibited significantly higher flow stress and flow strain, indicating distinct flow properties (Fig. 7C,D). Beyond the influence of oil droplet size on the interfacial area, the surface properties of the protein layer adsorbed on the droplets critically affected inter-droplet interactions. The augmented flow stress and flow strain observed in DeWPI0.25-stabilized HIPEs might be ascribed to the higher surface hydrophobicity and diminished zeta potential of DeWPI0.25, which has a lower DD, compared to those of DeWPI9. These characteristics foster intensified attractive interactions among oil droplets within the emulsion system.[51] Conversely, the excessive deamidation in DeWPI9 likely led to a highly charged protein layer, resulting in stronger electrostatic repulsion among the oil droplets and a weaker network structure. Notably, WPI-stabilized HIPEs showed the lowest G′, indicating the least elastic behavior, yet displayed the highest flow strain (approximately 66%) (Fig. 7D), suggesting significant deformability before breaking. Conversely, DeWPI-stabilized HIPEs, particularly DeWPI9-stabilizedHIPEs, not only likely exhibited higher stiffness because of their higher G', but also potentially showed increased brittleness as indicated by their lower flow strain compared to WPI-stabilized HIPEs.

Frequency sweep tests (Fig. 7E) revealed a slight, frequency-dependent increase in both the storage modulus (G') and loss modulus (G'') for the WPI- and DeWPI-stabilized HIPEs. Notably, G' remained higher than G'' throughout the measured frequency range, indicating a viscoelastic gel-like structure of the HIPEs.[52] The significantly higher G' observed in DeWPI-stabilized HIPEs compared to WPI-stabilized HIPEs aligned well with the findings from the amplitude sweep tests. Smaller droplets created a larger

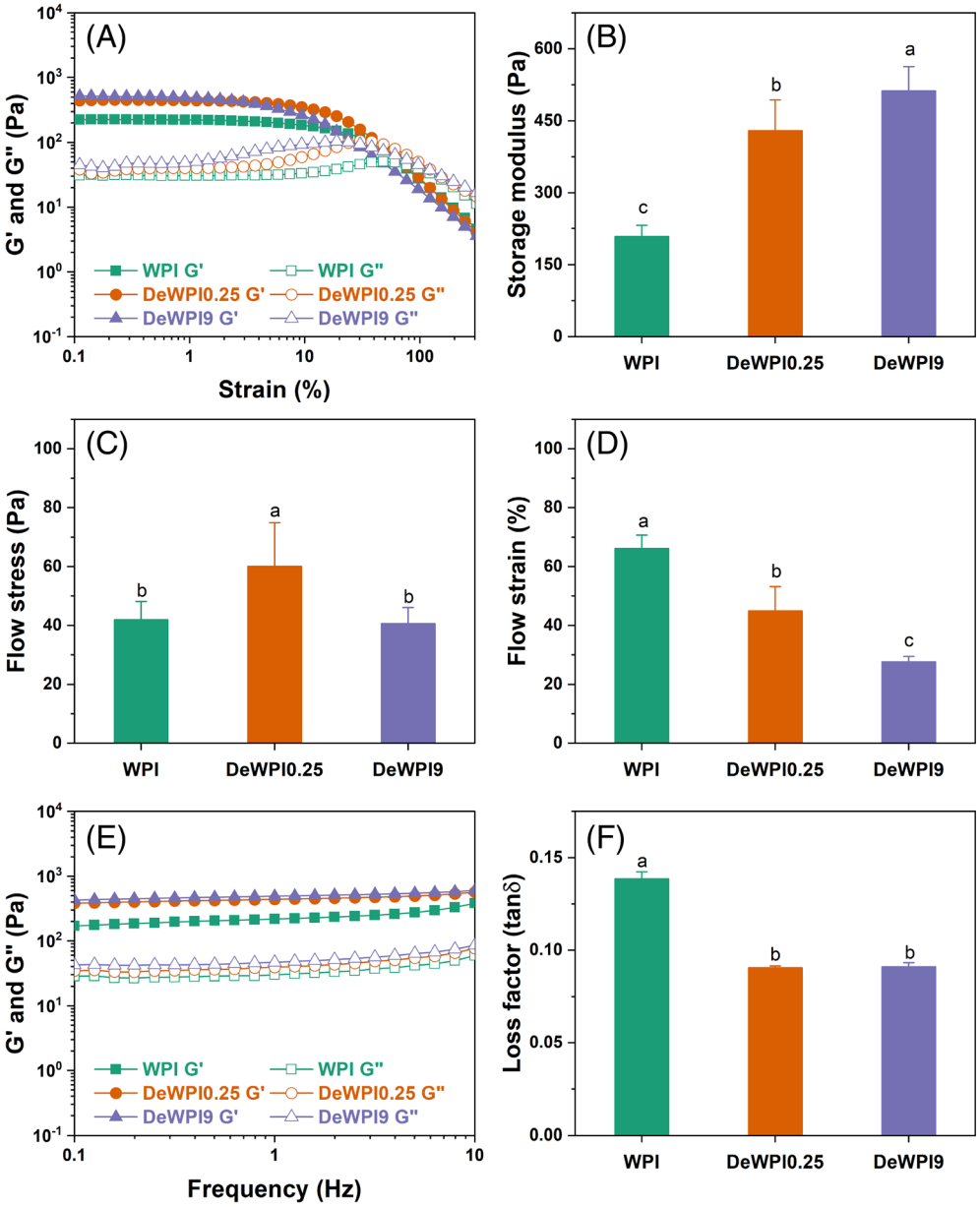

Figure 7. (A) Amplitude sweeps and (E) frequency sweeps for the high internal phase emulsions (HIPEs) stabilized by walnut protein isolates (WPI), DeWPI0.25 and DeWPI9. (B) Storage modulus, (C), flow stress, (D) flow strain and loss factor (F) of the HIPEs. Different letters indicate statistically significant differences ($P < 0.05$).

interfacial area, facilitating stronger inter-droplet interactions and contributing to a more rigid structure.[53] Additionally, the more compact interface resulted from the higher solubility of the deamidated proteins, further enhancing the overall strength of the HIPE network. The loss factor (tan δ), which reflects the ratio of G'' to G' and quantifies the energy dissipation within the material, further corroborated these observations. As shown in Fig. 7(F), WPI-stabilized HIPEs displayed a higher loss factor of approximately 0.14, whereas DeWPI-stabilized HIPEs exhibited loss tangents lower than 0.1, suggesting more elastic behavior.[54]

Physical stability of HIPEs stabilized by DeWPI

The long-term storage stability of the HIPEs was assessed and the results are shown in Fig. 8A,D. After storage for 28 days, the particle size and surface charge of the oil droplets in both the WPI- and DeWPI-stabilized HIPEs showed no significant alterations. Rheological analysis (see Supporting information, Fig. S5A–C) indicated that the G' of the WPI-stabilized HIPEs also remained unchanged after storage. The G' of DeWPI-stabilized HIPEs slightly increased. These results suggest that all HIPE formulations maintained their structural integrity and elastic properties during storage, indicating good overall stability.

The stability of the HIPEs against thermal stress was evaluated by heating at 60 and 90 °C. As shown in Fig. 8(B), heating at 60 and 90 °C caused a significant increase in the $d_{4,3}$ values of the WPI-stabilized HIPEs. By contrast, the DeWPI-stabilized HIPEs maintained their original $d_{4,3}$ values after treatment at 60 °C. However, at 90 °C, both DeWPI0.25- and DeWPI9-stabilized HIPEs exhibited a substantial increase in the measured $d_{4,3}$ values. Notably, as shown in the Supporting information (Fig. S6A), the size of

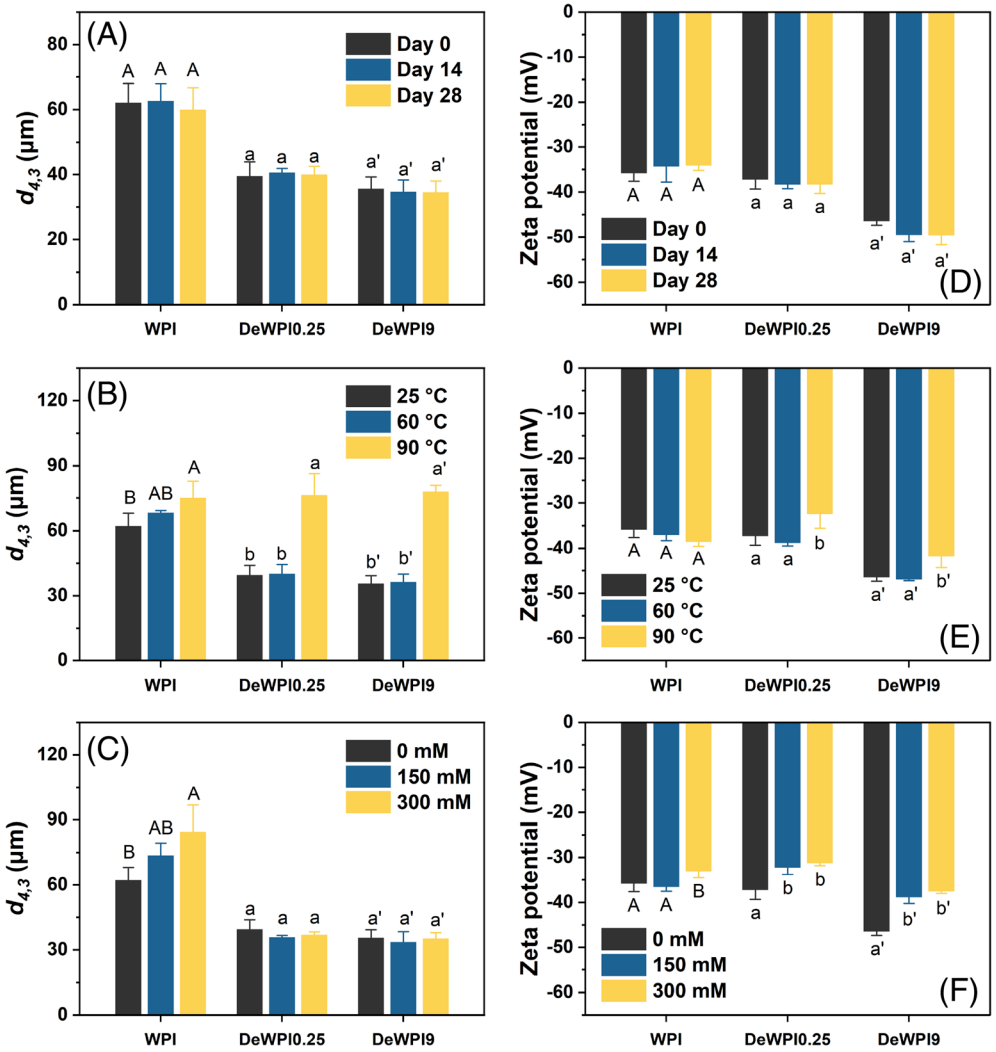

Figure 8. The influence of long-term storage (A,D), heat treatment (B,E) and high ionic strength (C,F) on the volume-weighted mean diameter ($d_{4,3}$) and zeta potential of oil droplets in the high internal phase emulsions (HIPEs) stabilized by walnut protein isolates (WPI), DeWPI0.25 and DeWPI9. Different letters indicate statistically significant differences ($P < 0.05$).

the individual oil droplets in the emulsions remained unchanged, suggesting that this increase is primarily a result of enhanced oil droplet flocculation.[53] Heating at 60 °C did not significantly affect the surface charge of the oil droplets in the WPI- and DeWPI-stabilized HIPEs. However, heating at 90 °C resulted in a decrease in the zeta potential of DeWPI-stabilized HIPEs (Fig. 8E). This decrease in electrostatic repulsion might further contribute to the observed oil droplet flocculation at high temperatures. As shown in the Supporting information (Fig. S5D–F), heating at 60 °C had minimal impact on the rheological profiles of both the WPI- and DeWPI-stabilized HIPEs. However, after heating at 90 °C, WPI-stabilized HIPEs displayed a slight decrease in G', indicating a weakening of the network structure. Conversely, DeWPI-stabilized HIPEs exhibited a notable increase in G' and flow strain. The improved elasticity and flow behavior suggested a strengthening of the HIPE network and enhanced resistance to deformation upon heating at 90 °C, primarily as a result of heat-induced protein unfolding. The unfolded proteins could expose buried hydrophobic patches, promoting stronger interactions between protein layers surrounding adjacent oil droplets. In addition, the formation of intermolecular disulfide bonds and subsequent covalent association of oil droplets might also occur, especially at high temperatures.[55,56] This could lead to greater entanglement between oil droplets and a denser protein layer at the interface, ultimately resulting in a more rigid network structure. In line with these findings, Dai *et al.*[51] reported that heat treatment increased G' in myofibrillar protein-stabilized HIPEs, potentially due to enhanced interactions such as hydrophobic interactions.

To evaluate the impact of ionic strength on emulsion stability, HIPEs were formulated with varying NaCl concentrations (150 and 300 mM). As shown in Fig. 8(C), WPI-stabilized HIPEs exhibited a significant increase in $d_{4,3}$ from 62 to 84 μm with 150–300 mM NaCl, whereas DeWPI-stabilized HIPEs displayed greater resistance to the effects of ionic strength and maintained their original droplet size. Optical microscopy images (see Supporting information, Fig. S6B) confirmed the presence of larger oil droplets in the WPI-stabilized HIPEs with the addition of NaCl. As expected, the high salt concentration effectively screened the surface charges of the oil droplets, as evidenced by the significant reduction in zeta potential observed for all HIPE samples (Fig. 8F). The greatly decreased G' of WPI-stabilized HIPEs could be connected with the larger oil droplet sizes, probably because

of the further decreased solubility of WPI in the presence of high concentrations of salt. By contrast, DeWPI-stabilized HIPEs displayed a slight change in G' but a notable increase in flow strain (see Supporting information, Fig. S5G–I). This enhanced flow behavior suggested a strengthening of the internal network structure, possibly as a result of increased inter-droplet interactions through hydrophobic interactions at high ionic strength, enabling the HIPEs to resist greater deformation. A previous study attributed the increased strength of HIPEs at high ionic strength to particle coagulation induced by electrostatic shielding.[57]

CONCLUSIONS

With the growing consumer demand for plant-based alternatives, improving the functionality of plant proteins, particularly their solubility and emulsifying properties, is an essential area of research for the food industry. The present study employed enzymatic deamidation to convert glutamine residues in walnut proteins to glutamate ones, resulting in a significant enhancement of their solubility. Furthermore, the DD played a crucial role in modulating the surface hydrophobicity and zeta potential of WPI. These modifications further significantly influenced their ability to stabilize LIPEs and HIPEs. The LIPEs stabilized by WPI or DeWPI0.25 exhibited lower emulsion stability than those stabilized by DeWPI9. Interestingly, DeWPI0.25-stabilized HIPEs displayed greater resistance to deformation and stress than DeWPI9-stabilized HIPEs. Both DeWPI0.25- and DeWPI9-stabilized emulsions demonstrated good stability against heating, high ionic strength and long-term storage. These findings highlight the potential of enzymatic deamidation as a valuable strategy to significantly improve the solubility and emulsifying ability of WPI, facilitating the utilization of walnut protein resources in the food industry. Future research could explore the gelation and foaming properties of deamidated WPI. Unveiling these functionalities could further expand the potential applications of WPI in various food product formulations.

ACKNOWLEDGEMENTS

We acknowledge the Center for Instrumental Analysis, School of Food Science and Bioengineering, Xihua University, for providing technical assistance. We thank AJE (https://www.aje.com) for linguistic assistance.

DATA AVAILABILITY STATEMENT

The data that support the findings of this study are available from the corresponding author upon reasonable request.

FUNDING

This work was supported by the National Natural Science Foundation of China (Grant No. 31670160) and the Talent Introduction Project of Xihua University (No. Z201028).

CONFLICTS OF INTEREST

The authors declare that they have no conflicts of interest.

SUPPORTING INFORMATION

Supporting information may be found in the online version of this article.

REFERENCES

1 Akharume FU, Aluko RE and Adedeji AA, Modification of plant proteins for improved functionality: a review. *Compr Rev Food Sci Food Saf* **20**: 198–224 (2021).
2 Gao K, Rao J and Chen B, Plant protein solubility: a challenge or insurmountable obstacle. *Adv Colloid Interface Sci* **324**:103074 (2024).
3 Zhao Y, He W, Zhao S, Jiao T, Hu H, Li J *et al*., Advanced insights into walnut protein: structure, physiochemical properties and applications. *Foods* **12**:3603 (2023).
4 Sze-Tao KWC and Sathe SK, Walnuts (*Juglans regia* L): proximate composition, protein solubility, protein amino acid composition and proteinin vitro digestibility. *J Sci Food Agric* **80**:1393–1401 (2000).
5 Liu F, Wang X, Zhao X, Hu H, Chen F and Sun Y, Surface properties of walnut protein from AOT reverse micelles. *Int J Food Sci Technol* **49**:626–633 (2014).
6 Li S, Liu Z, Hei X, Wu C, Ma X, Hu H *et al*., Effect of physical modifications on physicochemical and functional properties of walnut protein. *Foods* **12**:3709 (2023).
7 Zhang M, Cai S, Wang O, Zhao L and Zhao L, A comprehensive review on walnut protein: extraction, modification, functional properties and its potential applications. *J Agric Food Res* **16**:101141 (2024).
8 Kong X, Zhang L, Lu X, Zhang C, Hua Y and Chen Y, Effect of high-speed shearing treatment on dehulled walnut proteins. *LWT* **116**:108500 (2019).
9 Zhu Z, Zhu W, Yi J, Liu N, Cao Y, Lu J *et al*., Effects of sonication on the physicochemical and functional properties of walnut protein isolate. *Food Res Int* **106**:853–861 (2018).
10 Qin Z, Guo X, Lin Y, Chen J, Liao X, Hu X *et al*., Effects of high hydrostatic pressure on physicochemical and functional properties of walnut (*Juglans regia* L.) protein isolate. *J Sci Food Agric* **93**:1105–1111 (2013).
11 Mao X, Wang D, Sun L, Zhang J and Wu Q, Effect of peroxyl-radicals-induced oxidative modification in the physicochemical and emulsifying properties of walnut protein. *J Am Oil Chem Soc* **98**:903–910 (2021).
12 Ullah SF, Khan NM, Ali F, Ahmad S, Khan ZU, Rehman N *et al*., Effects of Maillard reaction on physicochemical and functional properties of walnut protein isolate. *Food Sci Biotechnol* **28**:1391–1399 (2019).
13 Ling M, Yan C, Huang X, Xu Y, He C and Zhou Z, Phosphorylated walnut protein isolate as a nanocarrier for enhanced water solubility and stability of curcumin. *J Sci Food Agri* **102**:5700–5710 (2022).
14 Yan C and Zhou Z, Solubility and emulsifying properties of phosphorylated walnut protein isolate extracted by sodium trimetaphosphate. *LWT* **143**:111117 (2021).
15 Huang X, Yan C, Lin M, He C, Xu Y, Huang Y *et al*., The effects of conjugation of walnut protein isolate with polyphenols on protein solubility, antioxidant activity, and emulsifying properties. *Food Res Int* **161**: 111910 (2022).
16 Wen C, Zhang Z, Cao L, Liu G, Liang L, Liu X *et al*., Walnut protein: a rising source of high-quality protein and its updated comprehensive review. *J Agric Food Chem* **71**:10525–10542 (2023).
17 Nikbakht Nasrabadi M, Sedaghat Doost A and Mezzenga R, Modification approaches of plant-based proteins to improve their techno-functionality and use in food products. *Food Hydrocoll* **118**:106789 (2021).
18 Liu X, Wang C, Zhang X, Zhang G, Zhou J and Chen J, Application prospect of protein-glutaminase in the development of plant-based protein foods. *Foods* **11**:440 (2022).
19 Zhang G, Ma S, Liu X, Yin X, Liu S, Zhou J *et al*., Protein-glutaminase: research progress and prospect in food manufacturing. *Food Biosci* **43**:101314 (2021).
20 Yong YH, Yamaguchi S, Gu YS, Mori T and Matsumura Y, Effects of enzymatic deamidation by protein-glutaminase on structure and functional properties of α-Zein. *J Agric Food Chem* **52**:7094–7100 (2004).
21 Immonen M, Myllyviita J, Sontag-Strohm T and Myllärinen P, Oat protein concentrates with improved solubility produced by an enzyme-aided ultrafiltration extraction method. *Foods* **10**:3050 (2021).
22 Jiang Y, Wang Z, He Z, Zeng M, Qin F and Chen J, Effect of heat-induced aggregation of soy protein isolate on protein-glutaminase deamidation and the emulsifying properties of deamidated products. *LWT* **154**:112328 (2022).
23 Kunarayakul S, Thaiphanit S, Anprung P and Suppavorasatit I, Optimization of coconut protein deamidation using protein-glutaminase

and its effect on solubility, emulsification, and foaming properties of the proteins. *Food Hydrocoll* **79**:197–207 (2018).
24 Fang L, Xiang H, Sun-Waterhouse D, Cui C and Lin J, Enhancing the usability of pea protein isolate in food applications through modifying its structural and sensory properties via deamidation by glutaminase. *J Agric Food Chem* **68**:1691–1697 (2020).
25 Temthawee W, Panya A, Cadwallader KR and Suppavorasatit I, Flavor binding property of coconut protein affected by protein-glutaminase: vanillin-coconut protein model. *LWT* **130**:109676 (2020).
26 Jiang Z, Sontag-Strohm T, Salovaara H, Sibakov J, Kanerva P and Loponen J, Oat protein solubility and emulsion properties improved by enzymatic deamidation. *J Cereal Sci* **64**:126–132 (2015).
27 Liu Y, Li X, Zhou X, Yu J, Wang F and Wang J, Effects of glutaminase deamidation on the structure and solubility of rice glutelin. *LWT* **44**: 2205–2210 (2011).
28 Cai Z, Wei Y, Shi A, Zhong J, Rao P, Wang Q *et al*., Correlation between interfacial layer properties and physical stability of food emulsions: current trends, challenges, strategies, and further perspectives. *Adv Colloid Interface Sci* **313**:102863 (2023).
29 Zhang M, Li X, Zhou L, Chen W and Marchioni E, Protein-based high internal phase Pickering emulsions: a review of their fabrication, composition and future perspectives in the food industry. *Foods* **12**:482 (2023).
30 Mao X and Hua Y, Composition, Structure and functional properties of protein concentrates and isolates produced from walnut (*Juglans regia* L.). *Int J Mol Sci* **13**:1561–1581 (2012).
31 Go K, Horikawa Y, Garcia R and Villarreal FJ, Fluorescent method for detection of cleaved collagens using *O*-phthaldialdehyde (OPA). *J Biochem Biophys Methods* **70**:878–882 (2008).
32 Hayakawa S and Nakai S, Relationships of hydrophobicity and net charge to the solubility of Milk and soy proteins. *J Food Sci* **50**:486–491 (2006).
33 Ventureira JL, Bolontrade AJ, Speroni F, David-Briand E, Scilingo AA, Ropers M-H *et al*., Interfacial and emulsifying properties of amaranth (*Amaranthus hypochondriacus*) protein isolates under different conditions of pH. *LWT* **45**:1–7 (2012).
34 Yong YH, Yamaguchi S and Matsumura Y, Effects of enzymatic deamidation by protein-glutaminase on structure and functional properties of wheat gluten. *J Agric Food Chem* **54**:6034–6040 (2006).
35 Ma S, Liu X, Zhou J, Sun Y, Zhang G, Li J *et al*., Characterization of high internal phase emulsions stabilized by protein glutaminase-deamidated wheat gluten. *LWT* **179**:114622 (2023).
36 Luo L, Deng Y, Liu G, Zhou P, Zhao Z, Li P *et al*., Enhancing solubility and reducing thermal aggregation in pea proteins through protein glutaminase-mediated deamidation. *Foods* **12**:4130 (2023).
37 Zhao J, Tian Z and Chen L, Effects of deamidation on aggregation and emulsifying properties of barley glutelin. *Food Chem* **128**:1029–1036 (2011).
38 Zhao J, Tian Z and Chen L, Effects of deamidation on structure and functional properties of barley hordein. *J Agric Food Chem* **58**: 11448–11455 (2010).
39 Fu W, Chen X, Cheng H and Liang L, Tailoring protein intrinsic charge by enzymatic deamidation for solubilizing chicken breast myofibrillar protein in water. *Food Chem* **385**:132512 (2022).
40 Liao L, Han X, Chen L, Ni L, Liu Z, Zhang W *et al*., Comparative characterization of the deamidation of carboxylic acid deamidated wheat gluten by altering the processing conditions. *Food Chem* **210**:520–529 (2016).
41 Lakowicz JR ed, *Protein Fluorescence. Principles of Fluorescence Spectroscopy*. Springer US, Boston, MA, pp. 529–575 (2006).
42 Woychik JH, Boundy JA and Dimler RJ, Wheat gluten proteins, amino acid composition of proteins in wheat gluten. *J Agric Food Chem* **9**: 307–310 (1961).
43 Wieser H, Koehler P and Scherf KA, Chemistry of wheat gluten proteins: qualitative composition. *Cereal Chem* **100**:23–35 (2023).
44 Liu G, Li J, Shi K, Wang S, Chen J, Liu Y *et al*., Composition, secondary structure, and self-assembly of oat protein isolate. *J Agric Food Chem* **57**:4552–4558 (2009).
45 Wang J, Zheng H, Zhang S, Li J, Zhu X, Jin H *et al*., Improvement of protein emulsion stability through glycosylated black bean protein covalent interaction with (−)-epigallocatechin-3-gallate. *RSC Adv* **11**:2546–2555 (2021).
46 Chen Y, Li L, Zhao X, Zeng X and Xu X, How environmental stresses affect the physical stability of oil in water emulsion prepared using pH-shifted myofibrillar protein? *LWT* **186**:115200 (2023).
47 McClements DJ, *Food Emulsions: Principles, Practices, and Techniques*, 3rd edn. CRC Press, Boca Raton (2015).
48 Gao H, Ma L, Cheng C, Liu J, Liang R, Zou L *et al*., Review of recent advances in the preparation, properties, and applications of high internal phase emulsions. *Trends Food Sci Technol* **112**:36–49 (2021).
49 Foudazi R, Qavi S, Masalova I and Malkin AY, Physical chemistry of highly concentrated emulsions. *Adv Colloid Interface Sci* **220**:78–91 (2015).
50 Zhang L, Zaky AA, Zhou C, Chen Y, Su W, Wang H *et al*., High internal phase Pickering emulsion stabilized by sea bass protein microgel particles: food 3D printing application. *Food Hydrocoll* **131**:107744 (2022).
51 Dai H, Sun Y, Feng X, Ma L, Chen H, Fu Y *et al*., Myofibrillar protein microgels stabilized high internal phase Pickering emulsions with heat-promoted stability. *Food Hydrocoll* **138**:108474 (2023).
52 Mezger TG, *The Rheology Handbook*, 4th edn. Vincentz Network, Hannover, Germany (2019).
53 Li X-L, Liu W-J, Xu B-C and Zhang B, Simple method for fabrication of high internal phase emulsions solely using novel pea protein isolate nanoparticles: stability of ionic strength and temperature. *Food Chem* **370**:130899 (2022).
54 Li Z, Xiong Y, Wang Y, Zhang Y and Luo Y, Low density lipoprotein-pectin complexes stabilized high internal phase pickering emulsions: the effects of pH conditions and mass ratios. *Food Hydrocoll* **134**:108004 (2023).
55 McClements DJ, Monahan FJ and Kinsella JE, Disulfide bond formation affects stability of whey protein isolate emulsions. *J Food Sci* **58**: 1036–1039 (1993).
56 Monahan FJ, McClements DJ and German JB, Disulfide-mediated polymerization reactions and physical properties of heated WPI-stabilized emulsions. *J Food Sci* **61**:504–509 (1996).
57 Feng T, Wang X, Wang X, Xia S and Huang Q, Plant protein-based antioxidant Pickering emulsions and high internal phase Pickering emulsions against broad pH range and high ionic strength: effects of interfacial rheology and microstructure. *LWT* **150**: 111953 (2021).

